

# Enantioselective separation of polychlorinated biphenyl atropisomers using chiral high-performance liquid chromatography

Peter Haglund

*Institute of Environmental Chemistry, Umeå University, S-901 87 Umeå, Sweden*

Received 7 June 1995; revised 15 August 1995; accepted 17 August 1995

---

## Abstract

Permethylated  $\beta$ -cyclodextrin derivatized silica was used as the chiral stationary phase in reversed-phase HPLC to separate the atropisomers of polychlorinated biphenyls (PCBs). The retention behaviour of 26 atropisomers was studied under optimum chromatographic conditions. Thirteen atropisomers could be completely resolved and six were partially separated. Among the atropisomers separated 14 are of environmental relevance since they do not enantiomerize at physiological temperatures. A retention behaviour study showed that tri-*ortho* PCBs, which lack “buttressing” chlorine substituents in the 3'-position, are difficult to separate. The best resolution was obtained for PCBs with 2,3,6-substitution in the less substituted biphenyl ring.

**Keywords:** Enantiomer separation; Atropisomer separation; Polychlorinated biphenyls

---

## 1. Introduction

It is known that biphenyls with large substituents in the *ortho* (2,2',6,6') positions can be chiral. The first example of a stable enantiomer due to restricted rotation, was 2,2'-dinitro-6,6'-diphenic acid reported by Christie and Kenner in 1922 [1]. Stereoisomers that are chiral solely as a result of restricted rotation about a single bond were designated as atropisomers by Kuhn [2].

Seventy-eight of the 209 polychlorinated biphenyls (PCBs) are also displaying axial chirality in their non-planar conformations. Many of these, however, rapidly enantiomerize [reversible interconversion of the (+)- and (-)-enantiomers] at room temperature as the energy barriers for rotation about the axial bond are low. An energy barrier of at least 20 kcal/mol is considered necessary for atropisomer isolation at room temperature [3]. Only nineteen

PCBs with three or four chlorines in the *ortho* positions may therefore exist as stable atropisomers in biota [4].

The structures, IUPAC numbering [5,6], and estimated energy barriers of enantiomerization [4] for the 19 atropisomeric PCBs are compiled in Table 1. For each of these PCBs there exist two stable atropisomers as shown in Fig. 1.

Atropisomers of PCB have previously been separated by enantioselective gas and liquid chromatographic techniques. Schurig and co-workers resolved atropisomeric PCBs 84, 91, 95, 132, 136, and 149 on capillary gas chromatography (GC) columns coated with immobilised per-methylated  $\beta$ -cyclodextrin (Chirasil-Dex) [7,8]. König et al. reported that octakis(2,6-di-O-methyl-3-O-pentyl)- $\gamma$ -cyclodextrin coated GC columns allow resolution of enantiomeric pairs of PCBs 45, 95, and 139 [9]. Recently, Hardt et al. reported the separation of the enantiomers of

Table 1

IUPAC numbering [5,6], systematic names, and energies of enantiomerization ( $\Delta E$ ) in kcal/mol for the studied PCB atropisomers

IUPAC	Species	$\Delta E$	IUPAC	Species	$\Delta E$
16	2,2',3-Trichlorobiphenyl		139	2,2',3,4,4',6-HxCB	25
40	2,2',3,3'-Tetrachlorobiphenyl (TeCB)		144	2,2',3,4,5',6-HxCB	25
45	2,2',3,6-TeCB	25	149	2,2',3,4',5',6-HxCB	25
82	2,2',3,3',4-Pentachlorobiphenyl (PeCB)		170	2,2',3,3',4,4',5-Heptachlorobiphenyl (HpCB)	
84	2,2',3,3',6-PeCB	29	171	2,2',3,3',4,4',6-HpCB	29
88	2,2',3,4,6-PeCB	25	174	2,2',3,3',4,5,6'-HpCB	29
91	2,2',3,4',6-PeCB	25	175	2,2',3,3',4,5',6-HpCB	29
95	2,2',3,5',6-PeCB	25	176	2,2',3,3',4,4',6-HpCB	58
128	2,2',3,3',4,4'-Hexachlorobiphenyl (HxCB)		180	2,2',3,4,4',5,5'-HpCB	
131	2,2',3,3',4,6-HxCB	29	183	2,2',3,4,4',5',6-HpCB	25
132	2,2',3,3',4,6'-HxCB	29	194	2,2',3,3',4,4',5,5'-Octachlorobiphenyl (OCB)	
135	2,2',3,3',5,6'-HxCB	29	196	2,2',3,3',4,4',5,6'-OCB	29
136	2,2',3,3',6,6'-HxCB	58	197	2,2',3,3',4,4',6,6'-OCB	58

PCBs 45, 84, 88, 91, 95, 131, 132, 135, 136, 139, 149, 174, 175, 176, and 183. However, in the latter case four different stationary phases were required to achieve this separation, viz. heptakis(2,6-di-O-methyl-3-O-pentyl)- $\beta$ -cyclodextrin, octakis(2,6-di-O-methyl-3-O-pentyl)- $\gamma$ -cyclodextrin, heptakis(2,3-di-O-methyl-6-O-*tert.*-butyldimethylsilyl)- $\beta$ -cyclodextrin, and heptakis(2,3-di-O-methyl-6-O-*tert.*-hexyldimethylsilyl)- $\beta$ -cyclodextrin [10]. A few atropisomeric PCBs have also been completely (PCB197) or partially (PCB88 and PCB139) separated by liquid chromatography on triacetylcellulose [11,12].

The atropisomeric PCBs that were separated or enriched by liquid chromatography on triacetylcellulose have been subjected to various toxicological tests. Püttmann et al. studied the *in vivo* induction of total cytochrome P-450 content, aminopyrine N-demethylase, and aldrin epoxidase in rats. The racemic PCB139 was found to be a potent phenobarbital-type inducer. (+)-PCB139 enhanced all test systems more potently than did (-)-PCB139. In contrast, the

racemic PCB197 (and its enantiomers) were only weak phenobarbital-type inducers of cytochrome P-450, and the potencies of the individual enantiomers were equal [13].

Rodman et al. used chicken embryo hepatocyte cultures *in vitro* to determine if chirality plays a role in the recognition events associated with the induction of cytochrome P-450, and in the accumulation of uroporphyrin (URO) [14]. The reported order of potency for cytochrome P-450 induction was PCB139 > PCB197  $\geq$  PCB88. The (+)- and (-)-enantiomers of both PCB88 and PCB197 had equal potencies, whereas (+)-PCB139 was more potent than (-)-PCB139. Racemic PCB197 was a much more potent inducer of ethoxyresorufin-O-deethylase (EROD) activity than either PCB88 or PCB139. EROD activity was induced to a higher extent by the (+)-enantiomers of all compounds. Benzphetamine N-demethylase (BPDM) activity was induced in the order PCB197  $\geq$  PCB139 > PCB88. The (-)-enantiomers were more potent than the (+)-enantiomers, except for PCB139, the (+)-enantiomer of which was more potent. (+)-PCB139 caused the greatest percentage URO accumulation.

PCBs are ubiquitous environmental pollutants and are well known to undergo bio-accumulation in biota. Part-per-million levels are commonly found in species at all levels of the food web, with the highest tissue concentrations in, e.g. humans, marine mammals, and birds of prey. Much effort has been invested to assess the environmental impact and health effects of these compounds. Unfortunately, the existence of stable atropisomeric PCBs has not been

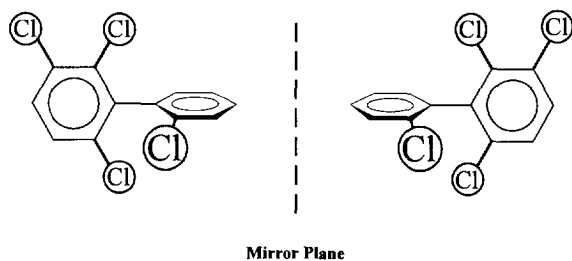


Fig. 1. Enantiomers of an atropisomeric PCB (PCB45).

considered in most of the toxicological studies which serve as the basis for the present risk evaluation of PCB. The recent discovery of the enantioselective biological properties of the PCB atropisomers has therefore aroused an increased concern among toxicologists. However, the limited availability of pure enantiomers currently restrains research efforts in the area of enantioselective toxicological testing. It appears that only three atropisomeric PCBs (discussed above) are presently available for toxicity studies.

The aim of the present study has therefore been to investigate if chiral high-performance liquid chromatography (HPLC) on permethylated  $\beta$ -cyclodextrin derivatized silica can be used to separate additional enantiomeric pairs of atropisomeric PCBs. Progress in this area might thus allow isolation of enantiomerically pure PCBs for careful toxicological investigation.

## 2. Experimental

### 2.1. Chemicals

The PCB reference standards were obtained from various sources: PCBs 45, 84, 91, 95, 131, 132, 135, 136, 170, 174, 175, 176, 196, and 197 were from Accustandard (New Haven, CT, USA); PCBs 16, 88, 128, and 180 were from Ultra Scientific (North Kingstown, RI, USA); PCB139 was from Dr. Ehrenstorfer (Augsburg, Germany); PCB149 was from Cambridge Isotope Laboratories (Andover, MA, USA); and PCBs 40, 82, 144, 171, 183, and 194 were kindly provided by the Institute of Applied Environmental Chemistry (Stockholm University, Stockholm, Sweden). All synthetic reference compounds were isomerically pure (>98%), although they were racemic. PCB standard solutions, 10 ng/ $\mu$ l, were prepared from iso-octane stock solutions by evaporation and reconstitution in an appropriate volume of methanol.

All solvents and chemicals used were of high quality. Gradient-grade methanol, reagent-grade triethylamine, and analytical-grade glacial acetic acid were obtained from Merck (Darmstadt, Germany). Water was purified using a Milli-Q Plus apparatus (Millipore, Bedford, MA, USA).

### 2.2. Optimisation of chromatographic conditions

The chromatographic conditions were theoretically optimised using a factorial experimental design, specifically a three-level face-centred central composite design (CCF), cf. Fig. 2 [15]. Three additional centre-points were included to estimate the experimental variance. In this type of experimental design a quadratic polynomial model is fitted to experimental results. The graphical meaning is that both planar and curved response surfaces can be accurately described. The experimental design was created, evaluated, and graphically illustrated using the MODDE software package (Umetri, Umeå, Sweden).

The three studied variables (i.e. experimental domains) included flow-rate (0.3 to 0.5 ml/min), buffer composition (0 to 1% triethylamine acetate buffer, pH 4, (TEAA) in 85% methanol), and column temperature (0°C to 30°C). The narrow flow-rate range was necessary since higher flow-rates would result in pressures exceeding the column pressure limit (300 bar) at 0°C, whereas lower flow-rates gave rise to excessive retention ( $t_R > 60$  min). The experimental design is shown in Table 2.

The order of the optimisation experiments was

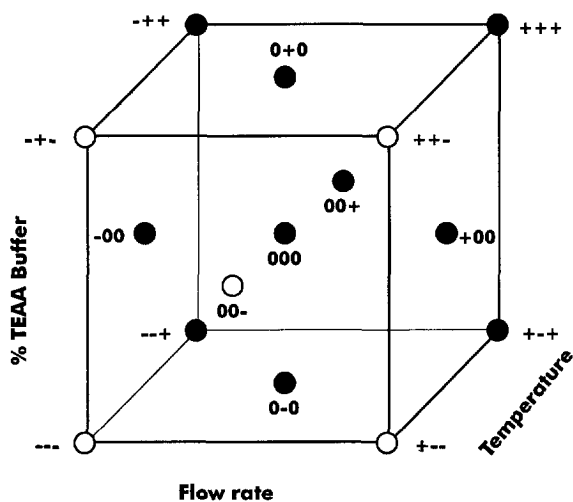


Fig. 2. Graphical representation of a three-level face-centred central composite (CCF) factorial experimental design. The plus, zero, and minus signs represents the high, intermediate and low level of the experimental variables, respectively.

Table 2

Experimental plan according to a three-level factorial design (+ = high level, 0 = intermediate level, and – = low level)

Experiment No.	Run order	Design		
		Flow-rate	% Buffer	Temperature
1	8	–	–	–
2	1	+	–	–
3	15	–	+	–
4	7	+	+	–
5	13	–	–	+
6	17	+	–	+
7	9	–	+	+
8	12	+	+	+
9	2	–	0	0
10	6	+	0	0
11	14	0	–	0
12	4	0	+	0
13	18	0	0	–
14	11	0	0	+
15	3	0	0	0
16	10	0	0	0
17	16	0	0	0
18	5	0	0	0

The high, intermediate, and low levels correspond to the following three combinations of experimental parameters: flow-rate, 0.5, 0.4, and 0.3 ml/min; % buffer, 1%, 0.5%, and 0% TEAA; temperature, 30, 15, and 0°C.

randomised to avoid systematic errors, cf. Table 2. A Hewlett-Packard 1050 liquid chromatographic system, consisting of a quaternary pump, an autosampler, and a variable-wavelength UV detector, was employed. The accompanying Hewlett-Packard Chemstation PC software was used for instrument control, data collection, and data analysis. Enantiomer separation was obtained by chromatography on two serially connected 250×4.6 mm Nucleodex  $\beta$ -PM columns (Macherey-Nagel, Düren, Germany). According to the manufacturer's documentation these columns are packed with 5  $\mu$ m Nucleosil 100 silica, which has been surface-modified with a covalently bonded chiral selector, permethylated  $\beta$ -cyclodextrin (PMCD). A Model 7950 column heater/chiller (Jones Chromatography, Hengoed, UK) was used to regulate the temperature of the chromatographic columns.

Aliquots (20  $\mu$ l) of the PCB174 standard solution were injected onto the PMCD columns, and the UV absorption of the eluent was monitored at 210 nm. The resulting peaks were integrated and three measures of performance, i.e. the number of theoretical plates ( $N$ ), selectivity ( $\alpha$ ), and resolution ( $R_s$ ), were calculated by the performance algorithm of the

Chemstation software. The number of theoretical plates was calculated on the first eluting atropisomer of the enantiomer pair.

### 2.3. Enantioselective separation of atropisomers of PCB

The retention behaviour of the PCB atropisomers was studied by injecting 20- $\mu$ l aliquots of the reference standard solutions. The chromatographic equipment and settings were the same as above, and the separations were performed under the optimum chromatographic conditions: 85% methanol at 0.4 ml/min, and a column temperature of 0°C (see Section 3).

## 3. Results and discussion

### 3.1. Optimisation of the chromatographic conditions

A response surface model was fitted, using the partial least square (PLS) algorithm, to the three response variables (number of theoretical plates,  $N$ , selectivity,  $\alpha$ , and resolution,  $R_s$ ). Three principal

components were found to be statistically significant, as determined by cross-validation. All experimental data fit the model, and the residual error sum of squares ( $R^2$ ) and prediction error sum of squares ( $Q^2$ ) values were satisfactory. The respective  $R^2$  and  $Q^2$  values were 0.992 and 0.860 for  $N$ , 0.984 and 0.736 for  $\alpha$ , and 0.964 and 0.781 for  $R_s$ .

The statistical data treatment revealed that the column temperature was by far the most important variable of the three studied response variables. The flow-rate ranked as the second most important

variable. The buffer composition was apparently not important, in fact the best chromatographic performances were obtained without added buffer. In Fig. 3 the response surfaces modelled for  $\alpha$ ,  $R_s$ , and  $N$ , as a function of column temperature and flow-rate, are shown. The response surface plot of  $N$  has been rotated 90° to enhance its presentation. In all three cases the buffer TEAA concentration was 0%.

As seen from the response surface plots, Fig. 3, all chromatographic properties are enhanced at lower flow-rates. The flow-rate dependence is most pro-

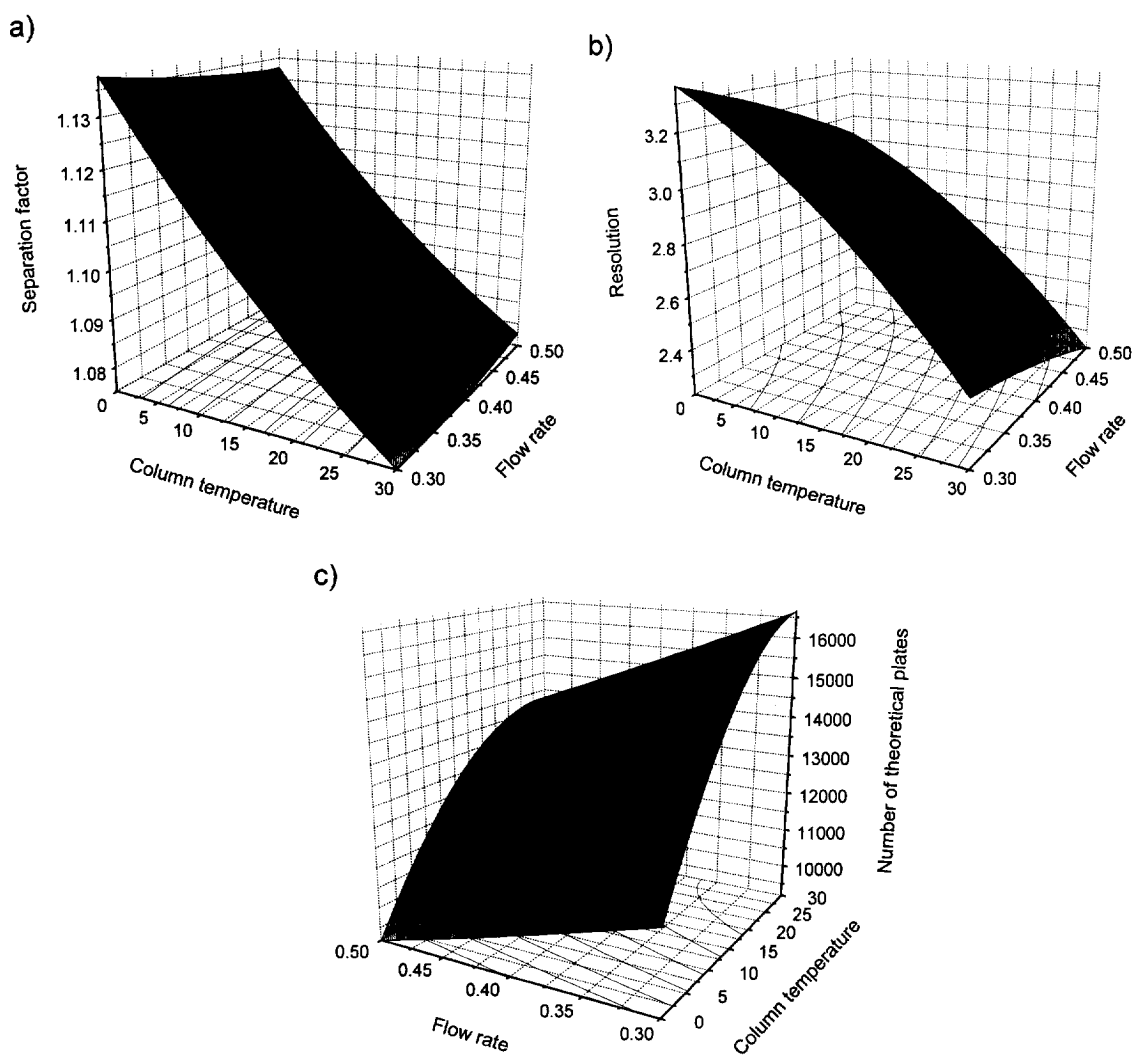


Fig. 3. Response surface plots describing (a) the separation factor ( $\alpha$ ), (b) the resolution ( $R_s$ ), and (c) the column efficiency ( $N$ ), as a function of column temperature and flow-rate. The buffer concentration was 0% TEAA in all cases. The HPLC instrumentation and experimental conditions are described in detail in Section 2.

nounced for  $N$ , but  $R_s$  is also influenced to a considerable extent.  $\alpha$  and  $R_s$  are enhanced when the column temperature is lowered. The inverse temperature dependence for  $\alpha$  is a well-known phenomenon in chiral HPLC and GC. This effect is attributed to the unique enthalpy-of-association values exhibited by each of the enantiomers within the diastereomeric inclusion complex, and which decrease with temperature [16]. In theory,  $\ln \alpha$  is proportional to  $1/T$ . The increase in  $\alpha$  at lower column temperatures (Fig. 3a) is however counteracted by  $N$ , which deteriorates with decreasing temperature (Fig. 3c). This can be explained in terms of the rate of diffusion in the mobile phase. The viscosity of the mobile phase increases as the column temperature decreases, and the diffusion is thereby obstructed.

Optimum chromatographic resolution was obtained at the lowest flow-rate of 0.3 ml/min, a column temperature of 0°C, and buffer strength of 0% TEAA. As the optimum is found at an extreme point, it is plausible that even better performances can be obtained outside the experimental domain. However, as seen in Fig. 3b, the response surface of  $R_s$  begins to level off at lower temperatures. Consequently, only marginal gain in resolution is expected by lowering the column temperature below 0°C. A further decrease in flow-rate would also give rise to increased chromatographic performance but, at the

same time (as pointed out earlier) would lead to prohibitively long retention times ( $t_R > 1$  h). It may be worthwhile to increase the flow-rate at the expense of resolution, in order to shorten the analysis time. The effect of such a measure can be predicted with the MODDE software. In Fig. 4 the calculated resolution, at four temperatures (20, 10, 0, and -10°C), is plotted versus the flow-rate. For the retention behaviour studies the following experimental conditions were therefore chosen: 85% methanol at 0.4 ml/min, and a column temperature of 0°C.

### 3.2. Separation of atropisomeric PCBs

The PMCD columns permitted separation of 14 of the 19 atropisomeric tri- and tetra-*ortho* PCBs (Table 3). In the calculations of the capacity ratio ( $k'$ ) the retention time for water has been used as  $t_M$ . The enantiomeric pairs of nine PCBs (PCBs 84, 131, 132, 135, 136, 174, 175, 176, and 196) were completely resolved ( $R_s \geq 2$  for all congeners). For the five remaining PCBs (PCBs 91, 95, 139, 171, and 197) only partial separation was obtained ( $R_s$  between 0.5 and 1). Representative chromatograms of both completely and partially resolved atropisomers are shown in Fig. 5.

It is worth noting that the PMCD and triacetylcellulose stationary phases display different selectivity

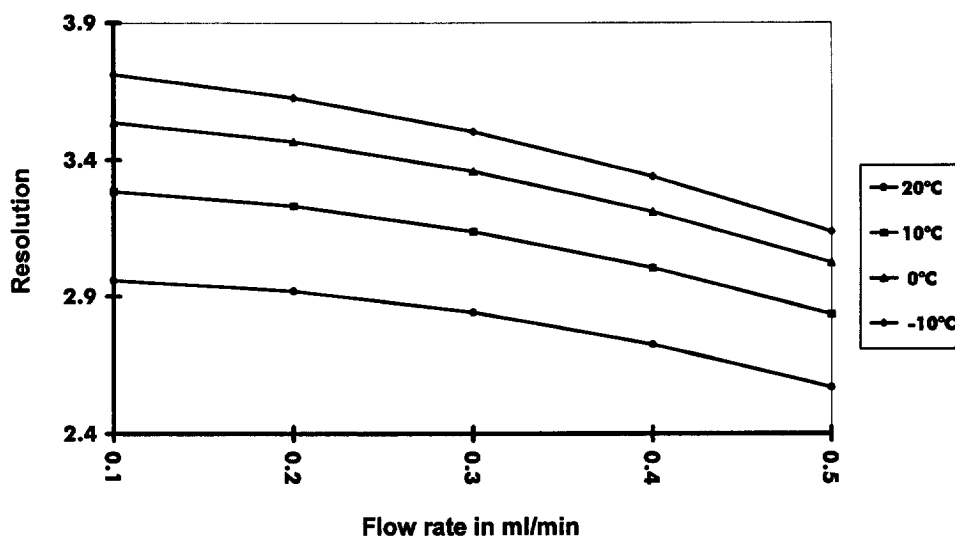


Fig. 4. Plot of the resolution ( $R_s$ ) as a function of flow-rate at four different temperatures.

Table 3  
Capacity factors ( $k'$ ), selectivity factors ( $\alpha$ ), and resolution ( $R_s$ ) for 26 atropisomeric PCBs on PMCD

IUPAC	Substitution	$k'_1$	$k'_2$	$\alpha$	$R_s$
16	23 - 2	2.06			
40	23 - 23	2.90	3.27	1.13	2.5
45	23 6 - 2	2.17			
82	234 - 23	3.73	4.10	1.10	1.6
84	23 6 - 23	2.70	3.18	1.18	3.5
88	234 6 - 2	2.77			
91	23 6 - 2 4	2.65	2.74	1.03	0.6
95	23 6 - 2 5	3.74	3.80	1.02	0.5
128	234 - 234	4.40	4.66	1.06	1.0
131	234 6 - 23	3.22	3.57	1.11	2.0
132	234 - 23 6	3.87	4.69	1.21	3.2
135	23 5 - 23 6	3.27	3.81	1.17	3.0
136	23 6 - 23 6	2.47	2.93	1.18	3.2
139	234 6 - 2 4	4.42	4.50	1.02	0.5
144	234 6 - 2 5	3.55			
149	23 6 - 2 45	3.62			
170	2345 - 234	5.94	6.41	1.08	1.2
171	234 6 - 234	4.32	4.48	1.04	0.7
174	2345 - 23 6	4.30	5.05	1.18	3.2
175	234 6 - 23 5	4.16	4.73	1.14	2.7
176	234 6 - 23 6	3.32	3.72	1.12	2.1
180	2345 - 2 45	6.29			
183	234 6 - 2 45	4.70			
194	2345 - 2345	7.91	8.56	1.08	0.8
196	2345 - 234 6	5.49	6.27	1.14	2.4
197	234 6 - 234 6	4.46	4.74	1.06	0.8

HPLC instrumentation and experimental conditions are described in detail in Section 2.

towards the PCB atropisomers. PMCD partially separates the atropisomers of PCB139 and PCB197, but not of PCB88. On the triacetylcellulose column the enantiomers of PCB88 and PCB139 were partially separated, and PCB197 were completely resolved [11,12].

Seven atropisomeric di-*ortho* PCBs (PCB16, PCB40, PCB82, PCB128, PCB170, PCB180, and PCB194) were studied in addition to the 19 tri- and tetra-*ortho* PCB atropisomers, cf. Table 1. All of these congeners are substituted in the 3-position, and all except PCBs 16 and 180 are also substituted in the 3'-position. This type of substitution is known to increase the energy of enantiomerization because of the so-called "buttressing effect" [3]. Normally, the *ortho* chlorines in di-*ortho* substituted PCBs are bent away from each other as the biphenyl approaches the planar transition-state. If this motion is impeded by a substituent in the adjacent position, then enantiomerization is significantly retarded. According to

Kaiser the increase in transition-state energy can be estimated at 2–5 kcal/mol for each buttressing chlorine atom [4]. Because of the buttressing effect these enantiomers were assumed to be stable enough to allow liquid chromatographic separation.

All of the studied di-*ortho* PCBs could be resolved except for PCB16 and PCB180. Most of the enantiomers were completely resolved ( $R_s > 1$ ;  $\alpha$ -values  $> 1.05$ ), whereas PCB194 was only partially resolved. Furthermore, in the chromatogram of PCB40 a plateau was observed between the peaks corresponding to the PCB enantiomers (Fig. 6). This plateau indicates that enantiomerization takes place within the chromatographic column despite the low column temperature (0°C), and the presence of two buttressing chlorine substituents in the structure [9,17]. The inability of the PMCD column to resolve the enantiomeric pairs of PCBs 16 and 180 (which only has one buttressing chlorine substituent) may therefore be attributed to a rapid enantiomerization

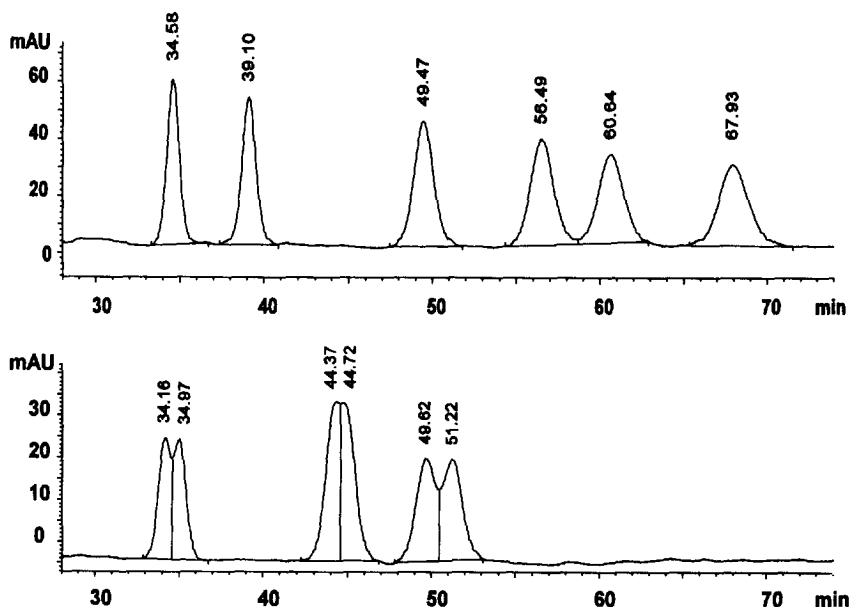


Fig. 5. UV chromatograms of fully (top) and partially (bottom) separated atropisomers of PCB. The fully resolved peaks originate from PCB84 (35 and 39 min), PCB174 (49 and 56 min), and PCB196 (61 and 68 min). The partially resolved peaks are from PCB91 (ca. 34 min), PCB95 (ca. 44 min), and PCB171 (ca. 50 min). The HPLC instrumentation and experimental conditions are described in detail in Section 2.

of the two enantiomeric forms. For the other PCBs (with two buttressing chlorine substituents) no such effect was observed. Further investigations are presently being undertaken to determine if any of these di-*ortho* PCBs is stable enough to resist enantio-merization at environmentally relevant temperatures.

### 3.3. Retention behaviour and enantioselectivity of atropisomeric PCBs

When cyclodextrin (CD)-based stationary phases are used under reversed-phase conditions, viz. with

aqueous mobile phases, the basic mechanism of retention is referred to as inclusion, or host-guest, complexation. This mechanism involves the attraction of an apolar molecule or segment to the apolar cavity of the CD molecule. At the large opening of the toroid there are a large number of secondary hydroxyl (or hydroxy derivative) groups which act as an energy barrier for entering polar molecules or segments. When a hydrophobic solute has entered the CD cavity chiral recognition is accomplished by interactions (attractive or repulsive) of substituents on or near the stereogenic centre with the 2- or

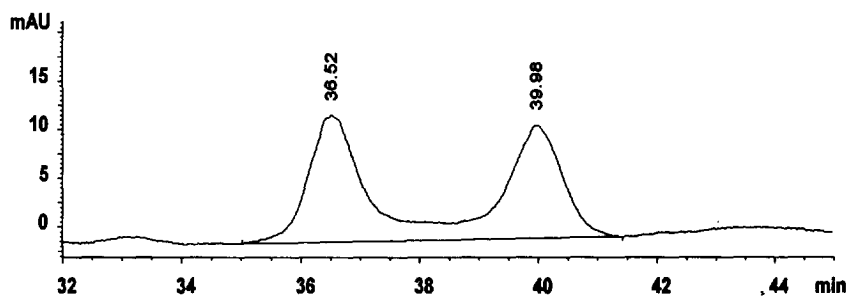


Fig. 6. UV chromatogram of PCB40. Note the plateau between the peaks, indicating partial enantiomerization within the HPLC column. The HPLC instrumentation and experimental conditions are described in detail in Section 2.



3-position hydroxyl (or hydroxy derivative) groups at the rim of the cavity [18]. Retention and chiral recognition in inclusion chromatography are thus dependent on the size, shape, and functionality of the solutes.

The retention of the PCBs in reversed-phase HPLC is expected to depend on the number of chlorine substituents. This, in fact, seems to be the case, since the trichloro-substituted PCB16 eluted first, and the following PCBs eluted according to the degree of chlorination (see Fig. 7). The correlation between  $k'$  and number of chlorine substituents has a regression coefficient ( $r^2$ ) of 0.72.

Assuming that the most hydrophobic part of the PCB (in this case the most substituted ring) binds to the cavity of the CD molecule, it is possible to study how the substitution pattern of the other ring affects  $\alpha$ , cf. Fig. 8. If there is an equal number of chlorine substituents on the biphenyl rings and the rings are not equally substituted it is thus not obvious which ring will bind to the CD cavity. In these cases (PCBs 132, 135, and 196), the orientation that produces the most logical results with respect to all other data has been chosen.

The most striking outcome of such a comparison is that di- and tri-*ortho* PCBs without substitution in the 3-position of the less substituted ring are not separated (PCBs 16, 45, 88, 144, 149, 180, and 183), or are only partially separated (PCBs 91, 95, and

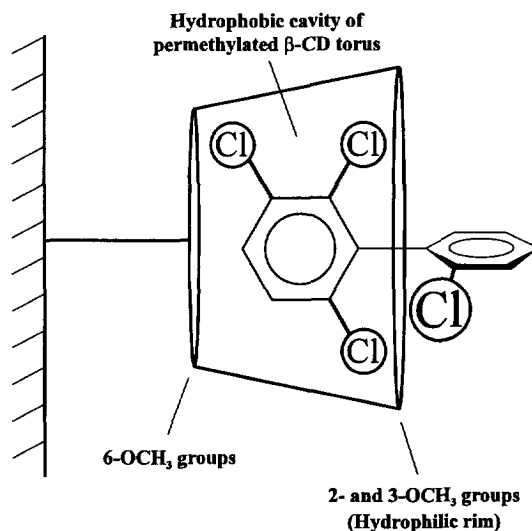


Fig. 8. Schematic representation of a host-guest complex between PCB45 and a covalently bonded PMCD molecule.

139). PCBs with at least the 2-, 3-, and 4-positions substituted (PCBs 128, 170, 171, 194, 196, and 197) are better separated with average  $\alpha$  and  $R_s$  values of 1.08 and 1.15, respectively. Substitution in the 2,3- or 2,3,5-positions (PCBs 40, 82, 131, and 175) results in still better enantiomer separation (average  $\alpha=1.12$ ; average  $R_s=2.2$ ). The best enantiomer separation (average  $\alpha=1.17$ ; average  $R_s=2.2$ ) is found among the PCBs which are substituted in the

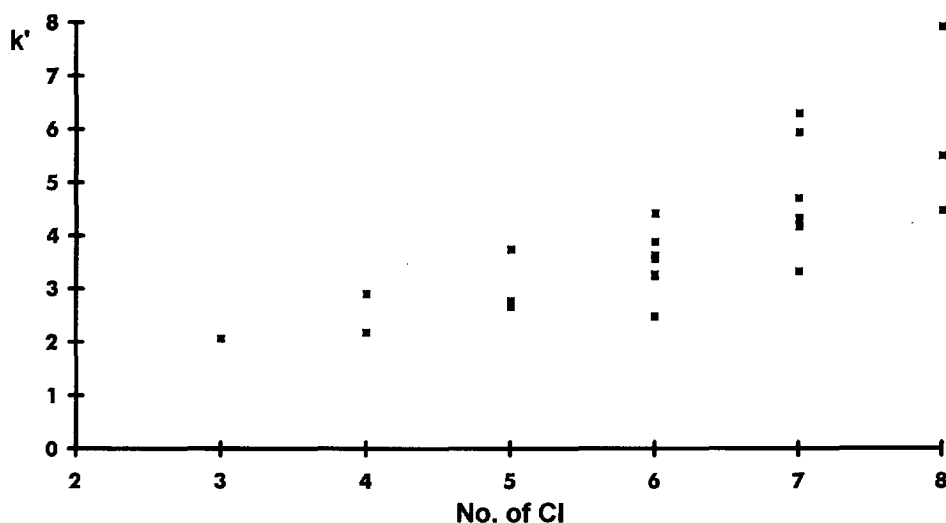


Fig. 7. Plot of capacity factors ( $k'$ ) on the PMCD column versus the number of chlorine substituents in the PCBs. The HPLC instrumentation and experimental conditions are described in detail in Section 2.

2,3,6-positions of the less substituted biphenyl ring (PCBs 132, 135, 136, 174, and 176).

The observed  $\alpha$  values correspond, however, to very small differences in complexation energies. A free energy difference of about 0.1 kcal/mol is sufficient to produce separation factors of 1.2 [16]. Such minute energy values are at least an order of magnitude lower than those normally associated with conformational changes in a molecule. It is therefore difficult to explain why some of the atropisomers are resolved, while others with similar structures are not. However, the factors pertaining to the inseparability of tri-*ortho* PCBs which lacks chlorine substituents in the 3'-positions are open to speculation. At least two explanations can be imagined: (1) the PCB molecules adopt a more planar conformation, since no buttressing chlorine substituent is present, and are thereby unable to interact strongly with the 2 and 3 methoxy groups of the PMCD; (2) the substituent in the 3'-position may be necessary for the formation of tight host-guest complexes, and for differentiation of the atropisomers. Needless to say, it is presently impossible to decide which of these models are the most likely, or if a combination of the proposed effects (1) and (2) is plausible.

#### 4. Conclusions

Chiral HPLC on PMCD has proven to be a rapid and useful tool for the separation of atropisomeric PCBs. Nine of the nineteen atropisomeric PCBs that are stable at room temperature were completely resolved whereas five were partially separated using this system. The five remaining atropisomeric PCBs could not be separated. Twelve of the nineteen, to our knowledge, have never before been separated by chiral liquid chromatography. These atropisomeric PCBs are now available for toxicological testing to determine if they exhibit enantioselective toxicological properties.

Furthermore, the enantiomer resolution was found to be determined by the substitution pattern of the less substituted biphenyl ring. The following order among the substitution patterns was observed: 2<2,4/2,5<2,3,4/2,3,4,5/2,3,4,6<2,3/2,3,5<2,3,6.

#### Acknowledgments

D.R. Zook is gratefully acknowledged for language revision in the final paper. This project was financially supported by the Swedish Environmental Protection Agency under the "Persistent Organic Pollutants" scientific program.

#### References

- [1] G.H. Christie and J. Kenner, *J. Chem. Soc.*, 121 (1922) 614.
- [2] R. Kuhn, in H. Freudenberg (Editor), *Molekulare Asymmetrie in Stereochemie*, Franz Deuticke, Leipzig, 1933, pp. 803–824.
- [3] E. Eliel, *Stereochemistry of Carbon Compounds*, McGraw-Hill, New York, 1962, Ch. 6.
- [4] K.L.E. Kaiser, *Environ. Pollut.*, 7 (1974) 93.
- [5] K. Ballschmitter and M. Zell, *Frezenius Z. Anal. Chem.*, 302 (1980) 20.
- [6] E. Schulte and R. Malisch, *Frezenius Z. Anal. Chem.*, 314 (1983) 545.
- [7] V. Schurig and A. Glausch, *Naturwissenschaften*, 80 (1993) 468.
- [8] A. Glausch, G.J. Nicholson, M. Fluck and V. Schurig, *J. High Resolut. Chromatogr.*, 17 (1994) 347.
- [9] W.A. König, B. Gehrcke, T. Runge and C. Wolf, *J. High Resolut. Chromatogr.*, 16 (1993) 376.
- [10] I.H. Hardt, C. Wolf, B. Gehrcke, D.H. Hochmuth, B. Pfaffenberger, H. Hühnenfuss and W.A. König, *J. High Resolut. Chromatogr.*, 17 (1994) 859.
- [11] A. Mannschreck, N. Pustet, L.W. Robertson, F. Oesch and M. Püttmann, *Liebigs Ann. Chem.*, (1985) 2101.
- [12] M. Püttmann, F. Oesch and L.W. Robertson, *Chemosphere*, 15 (1986) 2061.
- [13] M. Püttmann, A. Mannschreck, F. Oesch and L.W. Robertson, *Biochem. Pharmacol.*, 38 (1989) 1345.
- [14] L.R. Rodman, S.I. Shedlofsky, A. Mannschreck, M. Püttmann, A.T. Swim and L.W. Robertson, *Biochem. Pharmacol.*, 41 (1991) 915.
- [15] H. Martens and T. Naes, *Multivariate Calibration*, John Wiley and Sons, Chichester, 1989, pp. 305–307.
- [16] S. Allenmark, *Chromatographic Enantioseparation – Methods and Applications*, Ellis Horwood, New York, 2nd ed., 1992, p. 83.
- [17] M. Jung, M. Fluck and V. Schurig, *Chirality*, 6 (1994) 510.
- [18] ASPEC, *Cyclobond Handbook – A Guide to Using Cyclo-dextrin Bonded Phases*, Advanced Separation Technologies, Whippany, 1992.